**Supplementary Figure 1.** (*a)* Sequence conservation of mature miR-143 or miR-145 across species; red residues indicate variance. (*b*) Schematic of the genomic organization of miR-143 and miR-145 on mouse Chromosome 18; arrows indicate primers designed to amplify 1.7 kb transcript by reverse transcription of wt or *DGCR8*$^{null}$ cells. *Gapdh* was used as control for RNA loading and PCR performed with or without reverse transcriptase (RT). **(***c***)** Lateral view of *Islet1-cre; R26R-LacZ* lineage tracing by X-gal staining at E9.5. (*d*) FACS of YFP+ cells from E9.5 *Islet1-cre; R26R-YFP* embryos. (*e*) qPCR for levels of miR-143 and miR-145 in YFP+ cells relative to miR-16. N=3; *, $p<0.05$. Error bars indicate standard deviation (SD). (*f*) qPCR of miR-143 and miR-145 cardiac expression during embryonic development relative to whole embryo. (*g*) miRNA copy number per cell estimates at embryonic (E) days indicated. Expression of each miRNA in post-natal day 1 (P1) or P8 ventricles relative to liver is shown.

**Supplementary Figure 2.** (*a*) Percent identity between mouse and human across a 4.2 kb genomic region upstream of miR-143/145 cloned into an Hsp68-LacZ cassette. (*b*) β-Gal activity illustrating LacZ expression in the intestines of an E15.5 mouse embryo. (*c*) section of boxed area in (*b*) showing expression in smooth muscle (sm) of intestinal wall and in the vasculature. (*d*) qPCR of miR-143 and miR-145 in adult heart or aorta relative to liver. n=3; *, $p<0.05$. Error bars indicate standard deviation (SD).

**Supplementary Figure 3.** (*a*) Summary of the deletion and mutation analyses of the upstream enhancer region of miR-143/145. Asterisks (*) indicate mutations in the SRF or Nkx2.5 binding sites. Construct corresponds to images of β-gal activity focused on heart region (see Figs. 1, 2*a–e*). (*b*) Putative SRF and Nkx2.5 binding sites (green sequence)

within the 0.9 kb *cis*-regulatory element of miR-143 and miR-145. (*c)* LacZ expression of the 0.9 kb *cis*-acting regulatory element was present in the smooth muscle of the aorta, but a mutation of the SRF binding site eliminated enhancer activity. (*d*) Electrophoretic mobility-shift assay using radiolabeled probe for the SRF binding site. Competition with cold wild type (WT) or mutant (MT) probe indicates specificity of band.

**Supplementary Figure 4**. (*a*) Cross-sections from mice 21 days post-ligation of the left carotid artery compared to the contralateral right carotid artery without ligation (control). Immunohistochemistry revealed that smooth muscle (Sm) α-actin staining (red) was reduced in the ligated vessel compared to control. miR-143 and miR-145 expression (DIG-AP staining, dark purple) was markedly reduced in the ligated artery. (*b*) qPCR results of miR-29a, miR-143 or miR-145 expression in the border zone (BZ) or infarct zone (IZ) of mouse hearts after coronary ligation, relative to the non-ischemic distal zone (DZ) away from the infarct area (n=3). Error bars indicate SD.

**Supplementary Figure 5**. (*a*) qPCR of smooth muscle markers in fibroblasts treated with 250 ng Myocd with or without anti-miR-145 or (*b*) miR-143 (n=4). (*c*) qPCR of smooth muscle markers in fibroblasts treated with 50 ng of Myocd with or without miR-143 (n=4). (*d*) Immunocytochemistry of smooth muscle α-actin in Joma1.3 neural crest cells treated with tamoxifen (+4OHT) or miR-143. (*e*) qPCR of smooth muscle markers in neural crest cells (NCCs) with or without miR-143 (n=6). Slug and p75 represent markers of undifferentiated NCCs.

**Supplementary Figure 6**. (*a*) Sequence complementarity of two miR-143 or miR-145 binding sites in mouse *Elk-1* or *Myocd* 3′ UTRs, respectively. (*b*) qPCR of *Elk-1* mRNA levels (n=4). (*c*) Putative miR-145 binding site in the mouse 3′ UTR of *Klf4*. (*d*) qPCR of *Klf4* mRNA levels (n=4). (*e*) Putative binding site in the mouse 3´ UTR of *CamkII*-δ. (*f, g*) Relative luciferase activity of indicated 3′ UTRs downstream of luciferase (n=3). Predicted binding sites within the UTRs are indicated with residues complementary to miR-143 indicated in red capital letters. (*e*) Relative luciferase activity of indicated 3′ UTRs downstream of luciferase with or without miR-145 (n=3). Predicted binding sites within the UTRs are indicated with residues complementary to miR-145 indicated in red capital letters. No significant changes in luciferase activity were observed with any of these 3′ UTRs. Error bars indicate SD.

**Supplementary Figure 7**. (*a*) qPCR of miR-145 expression and (*b)* markers of smooth muscle differentiation in 9-day post-injured carotid arteries transduced with either lenti-control-GFP or lenti-miR-145-GFP viruses (n=3). Smooth muscle α-actin (Sm-α-actin); Sm-mhc, smooth muscle myosin heavy chain. Error bars indicate SD.

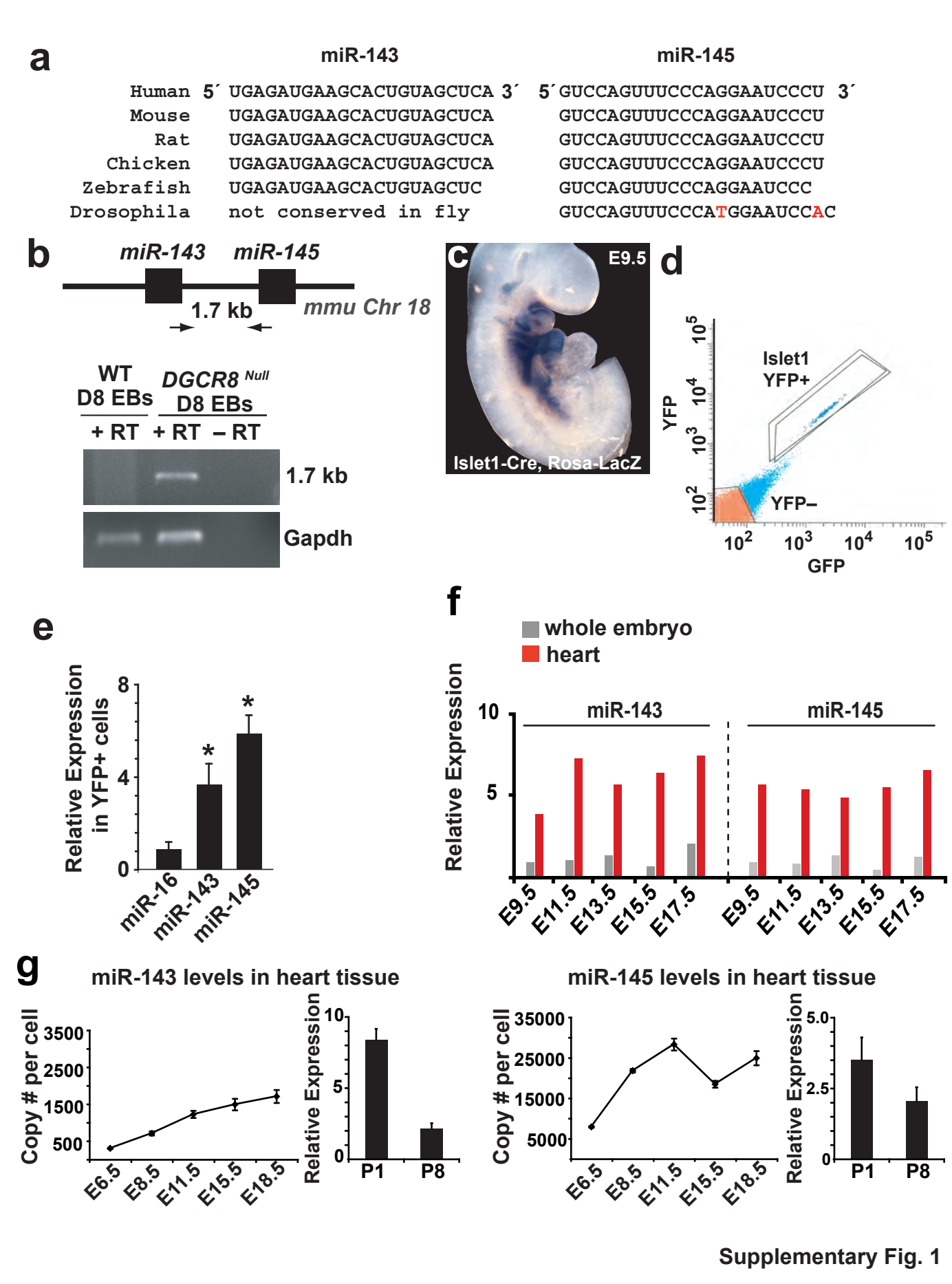


Supplementary Fig. 1

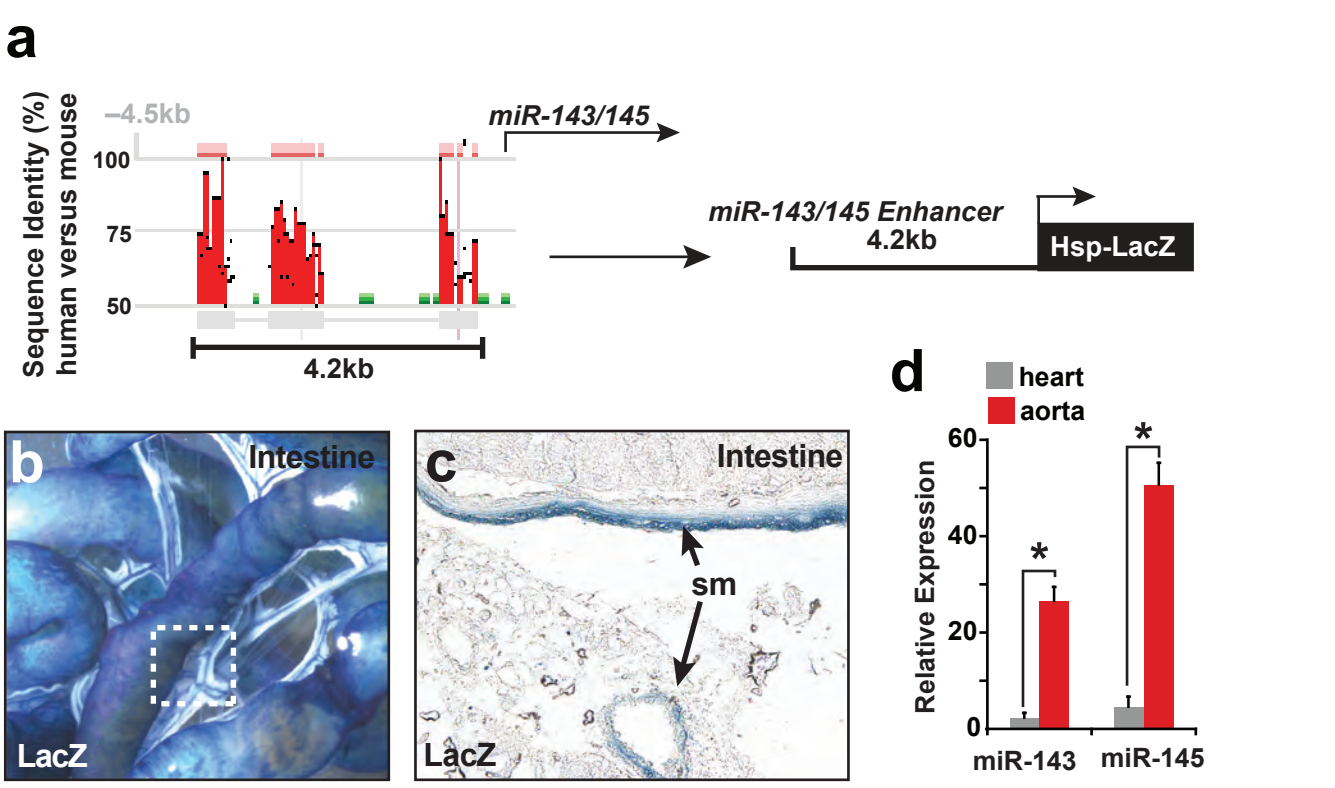


Supplementary Fig. 2

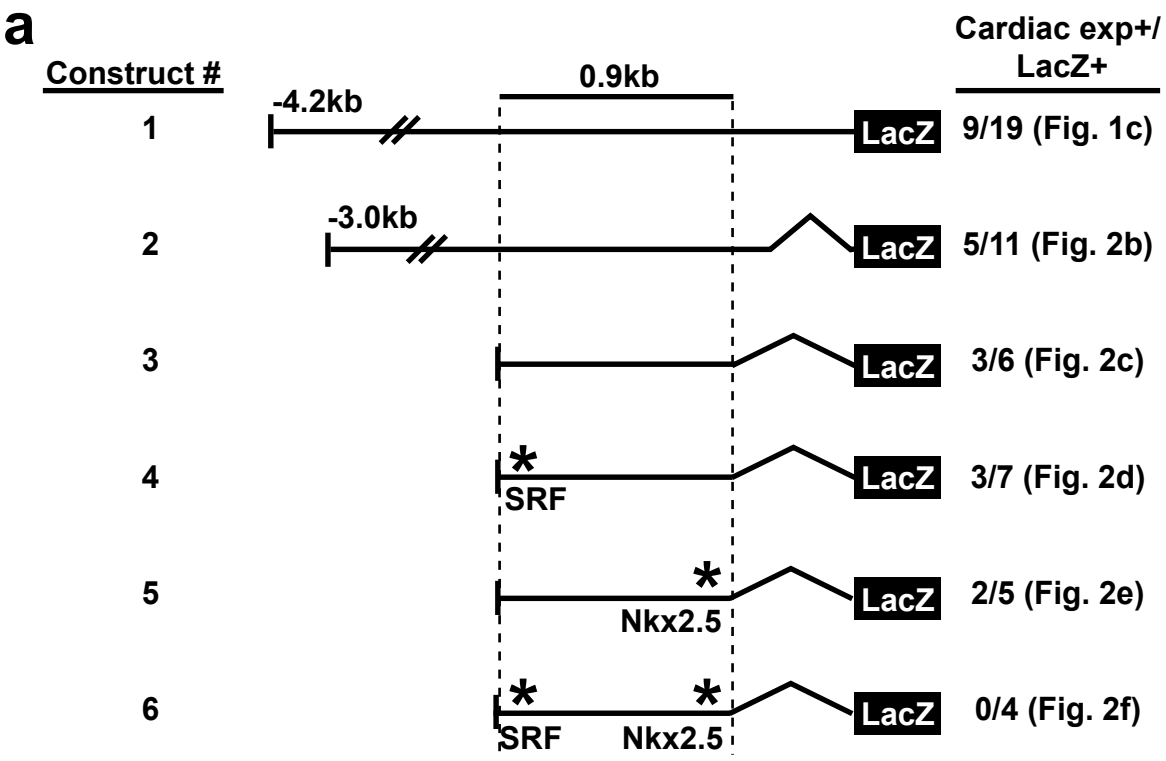


**b**

**SRF binding site**

GGGAGCAGCCTTGCCATATAAGGGCAGGAGCCCC **mmu chr 18: 61812158**

**SRF$^{mut}$ binding site**

GGGAGCAGCCTTGCTACCGCAGGGCAGGAGCCCC

**Nkx2.5 binding site**

GGGAAAGACTGCCAAGTGCTCGTGGCC **mmu chr 18: 61811308**

**Nkx2.5$^{mut}$ binding site**

GGGAAAGACTGCCGTGAGCTCGTGGCC

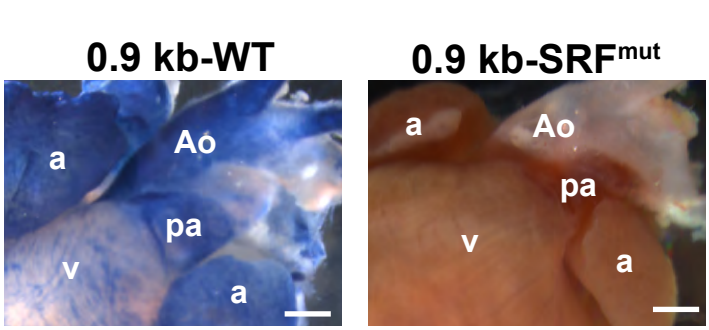


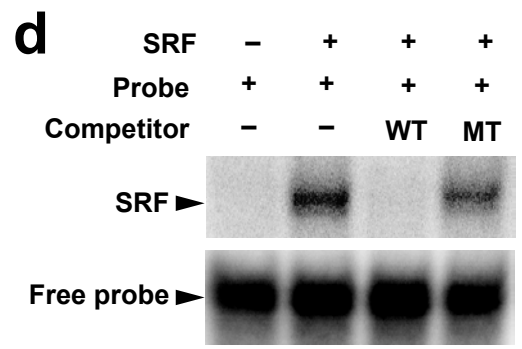


# Supplementary Fig. 3

# Supplementary Fig. 4

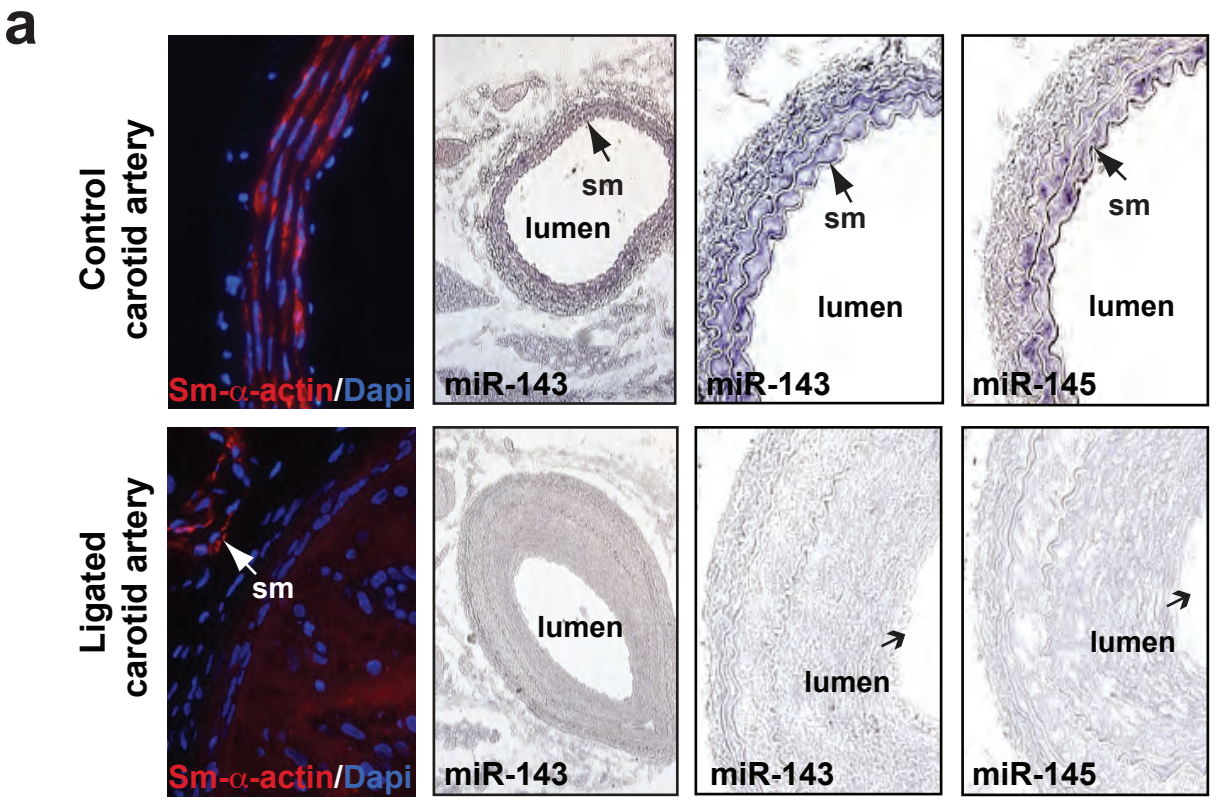


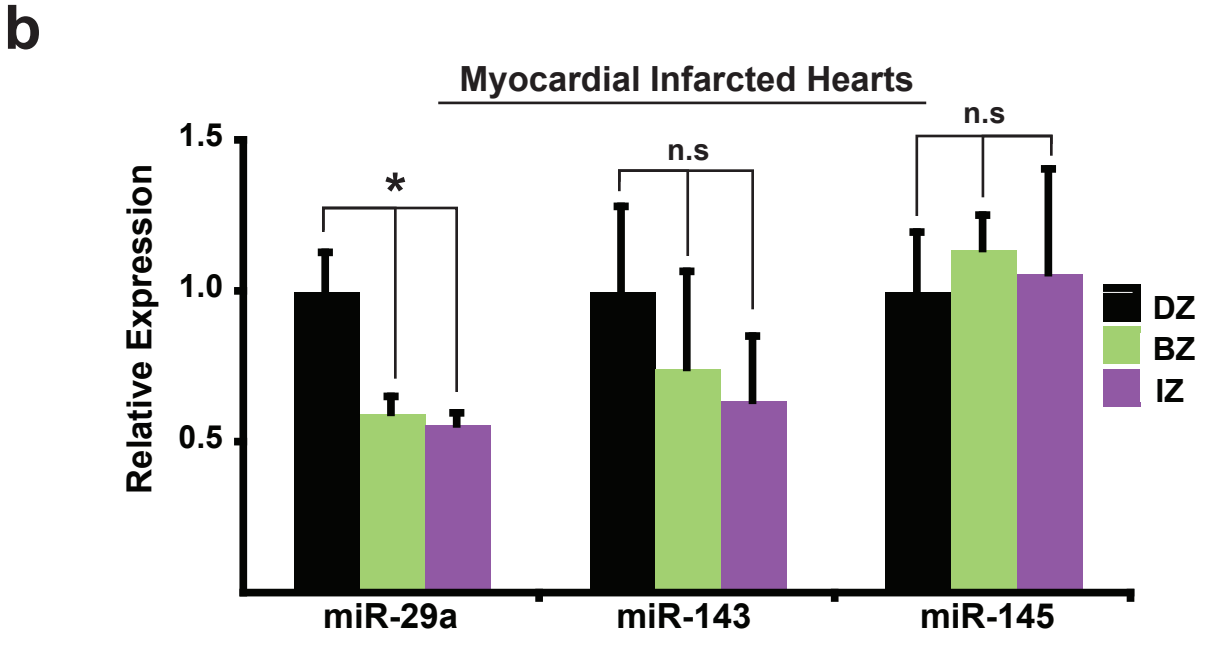

# Supplementary Fig. 5

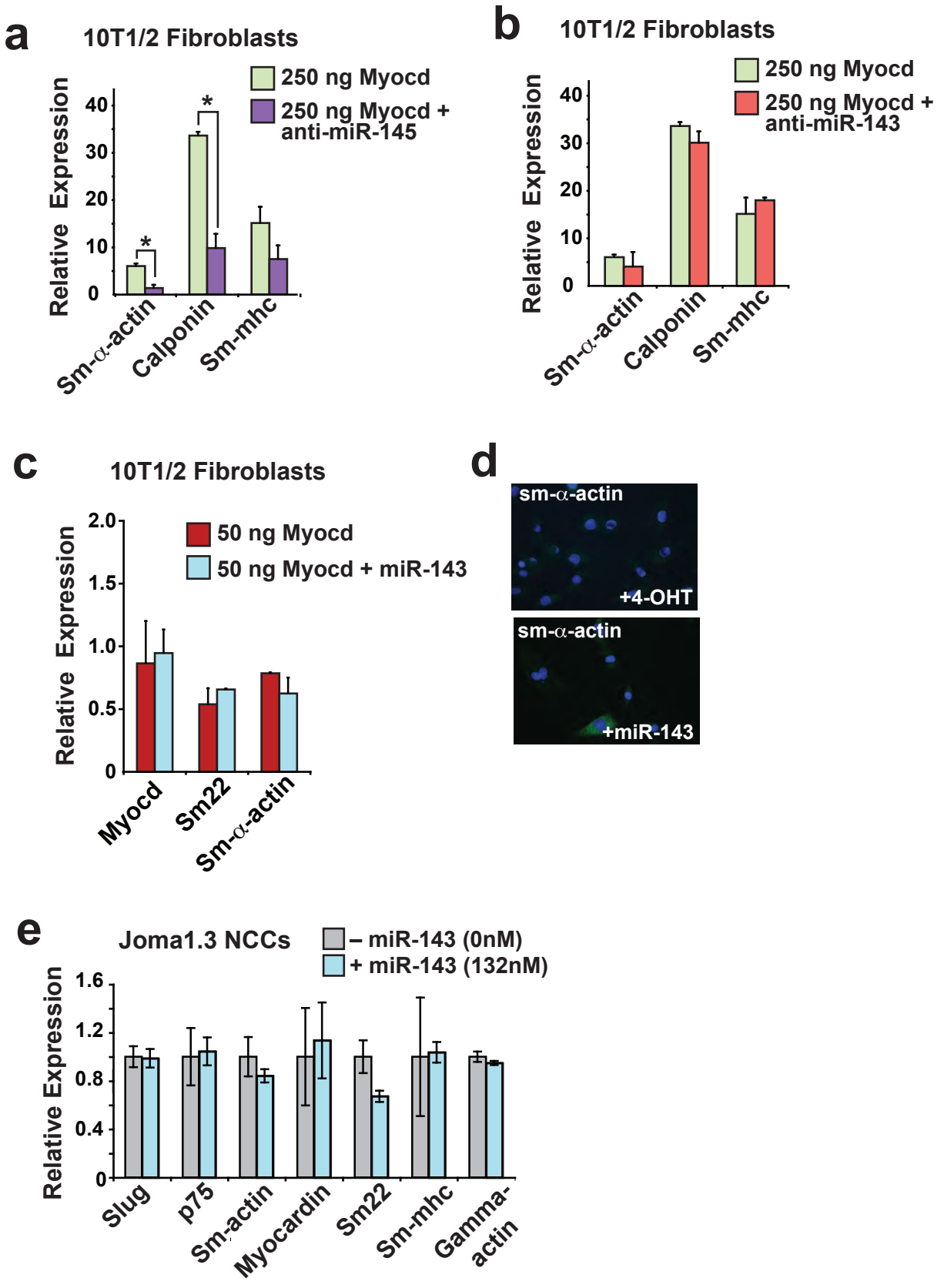

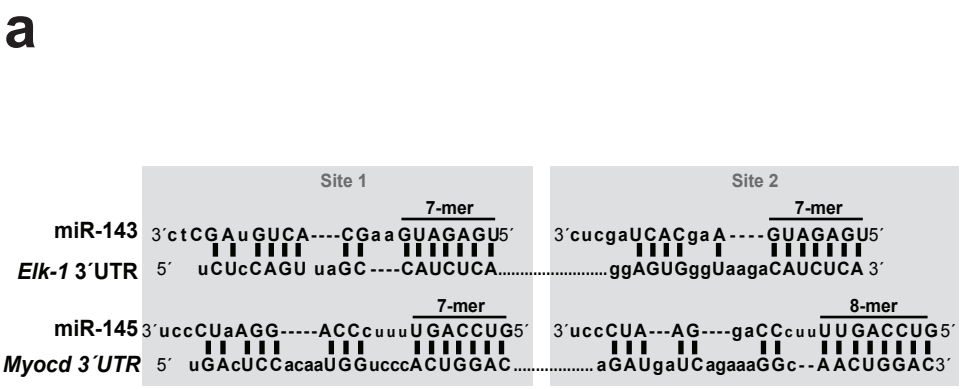


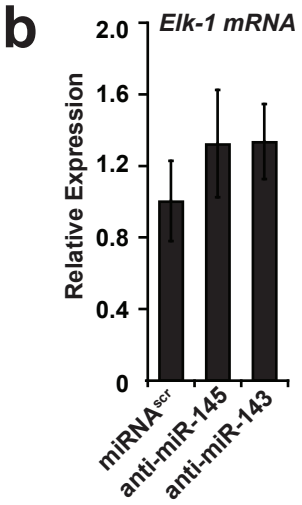


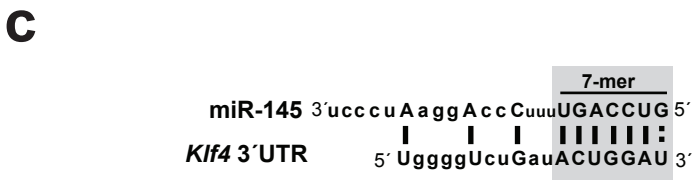


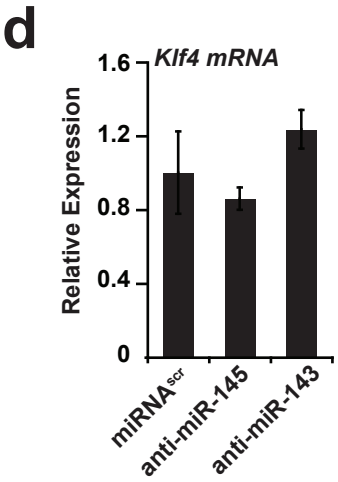


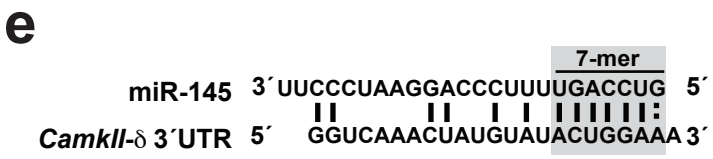


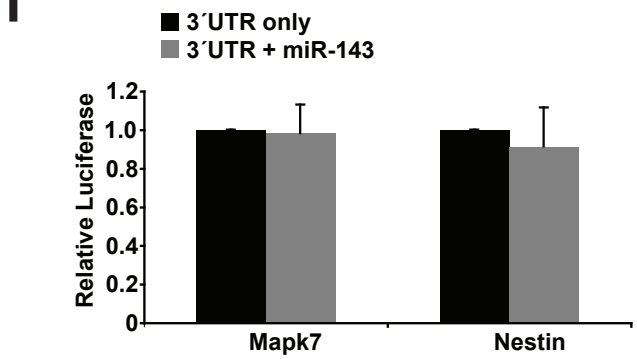


Mapk7 predicted binding site:
5′gGAGCaGCaaugaugAGUGaCUcucaUCAUCUCA 3′

Nestin predicted binding site:
5′uGAGUUACucUGCaggUUCAUCUCA 3′

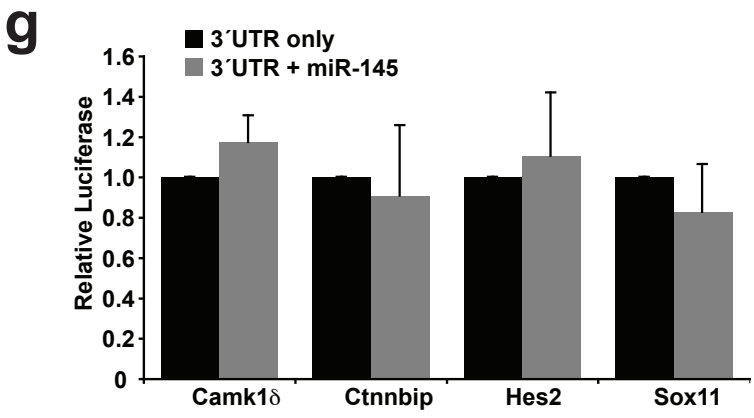


Camk1δ Target Scan predicted binding sites (2):
5′gugcaCCUGcaugaggACUGGAAg 3′
5′aaaaaUCaaGGuuucAACUGGAU 3′

Ctnnbip predicted binding site:
5′auuGGUUgCUuAAACUGGAa 3′

Hes2 predicted binding site:
5′guguaccUCUGcGGuACUGGAUg 3′

Sox11 Target Scan predicted binding sites (2):
5′agacagaaGGuuugaAACUGGAU 3′
5′uucaaaaacaGAAcgACUGGAAa 3′

# Supplementary Fig. 6

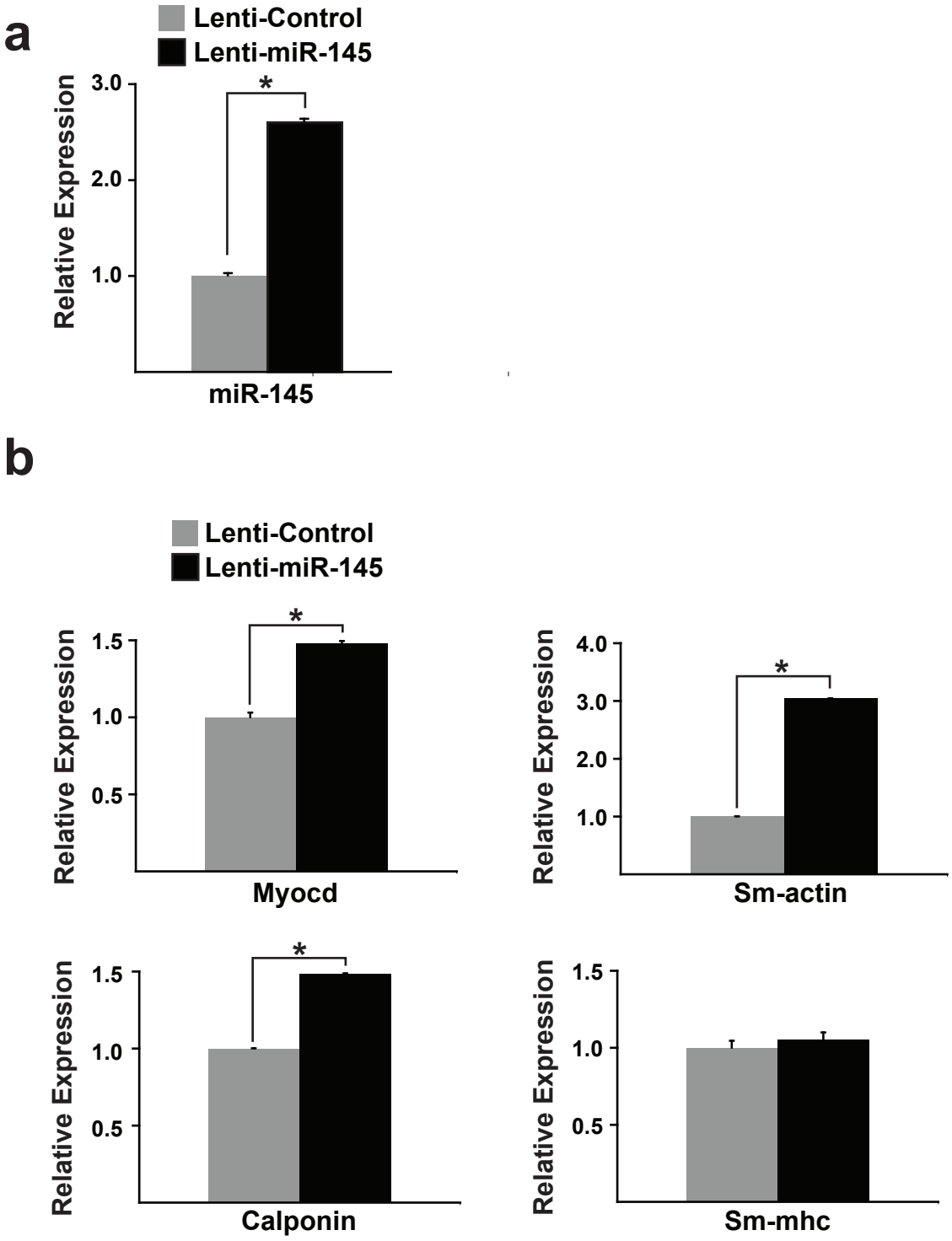


**Supplementary Fig. 7**